

OPERATION and PROPOSALS

1. Outline of the Accelerators

Two electron storage rings, namely the PF ring and the PF-AR, have been stably operated as dedicated light sources at the Photon Factory. The KEK linear accelerator with a maximum electron energy of 8 GeV is employed to inject electron beams into the rings. The full energy injection at 2.5 GeV is carried out at the PF ring, while it is necessary to ramp up the injection en-

ergy of 3 GeV to the operation energy of 6.5 GeV at the PF-AR.

The machine parameters of the rings and the calculated spectral performances are listed in **Table 1** and **Table 2**, respectively. The spectral distributions of synchrotron radiation (SR) from the bending magnets and the insertion devices are shown in **Fig. 1**.

Table 1: Principal beam parameters of the PF ring and PF-AR.

	PF ring	PF-AR
Energy	2.5 GeV	6.5 GeV
Natural emittance	34.6 nm rad	293 nm rad
Circumference	187 m	377 m
RF frequency	500.1 MHz	508.6 MHz
Bending radius	8.66 m	23.2 m
Energy loss per turn	0.4 MeV	6.66 MeV
Damping time		
Vertical	7.8 ms	2.5 ms
Longitudinal	3.9 ms	1.2 ms
Natural bunch length	10 mm	18.6 mm
Momentum compaction factor	0.00644	0.0129
Natural chromaticity		
Horizontal	-12.9	-14.3
Vertical	-17.3	-13.1
Stored current	450 mA	50 mA
Normal filling	212 bunches (53 X 4)	Single
Beam lifetime	20 h (at 450 mA)	13 h (at 50 mA)
Hybrid filling	Single (50 mA) + 131 bunches (400 mA)	
Beam lifetime	8 h (450 mA)	

Table 2: Calculated spectral performances of the bend source and all the insertion devices at the PF ring (2.5 GeV, 450 mA) and the PF-AR (6.5 GeV, 60 mA). λ_u : period length, N : number of the periods, L : length of undulator or wiggler, $G_y(G_x)$: minimum vertical (horizontal) gap height, $B_y(B_x)$: maximum vertical (horizontal) magnetic field, Type of magnet, H: hybrid configuration, S.C.: superconducting magnet, σ_x, σ_y : horizontal or vertical beam size, σ_x, σ_y : horizontal or vertical beam divergence, $K_y(K_x)$: vertical (horizontal) deflection parameter, D : photon flux density (photons/sec/mrad²/0.1%b.w.), B : brilliance (photons/sec/mm²/mrad²/0.1%b.w.), P_T : total radiated power. Different operating modes of undulator and wiggler are denoted by -U and -W, respectively

Name	E/I GeV/ImA	λ_u cm	N	L m	$G_y(G_x)$ cm	$B_y(B_x)$ T	Type of magnet	σ_x mm	σ_y mm	σ_x mrad	σ_y mrad	$K_y(K_x)$	ϵ_x/ϵ_c keV	D	B	P_T kW
PF 2.5/450																
Bend								0.41	0.059	0.178	0.012	4	5.38E+13	3.48E+14		
SGU#01		1.2	39	0.5	0.4	0.7	P(NdFeB)	0.6	0.012	0.088	0.029	0.78	4.56E+16	9.90E+17		0.4
U#02-1		6	60	3.6	2.8	0.4	H(NdFeB)	0.65	0.042	0.054	0.008	2.3	2.73E+17	1.55E+18		1.07
U#02-2		16	17	2.72	2.6	0.33(0.33)	P(NdFeB)	0.65	0.042	0.054	0.008	4.93(4.93)	9.53E+15	4.58E+16		0.53
SGU#03		1.8	26	0.5	0.4	1	P(NdFeB)	0.6	0.012	0.088	0.029	1.68	2.50E+16	5.44E+17		0.82
MPW#05-W		12	21	2.5	2.64	1.4	H(NdFeB)	0.71	0.045	0.078	0.009	16	2.22E+15	1.10E+16		8.83
U#13		7.6	47	3.6	2.3	0.74(0.51)	P(NdFeB)	0.74	0.02	0.094	0.019	5.28(3.65)	4.46E+16	3.10E+17		3.53
VW#14					5	5	S.C.	0.53	0.045	0.128	0.008	20.8	5.42E+13	3.59E+14		
SGU#15		1.76	27	0.5	0.4	0.97	P(NdFeB)	0.6	0.012	0.088	0.029	1.37	4.38E+15	9.44E+16		0.75
U#16-1 & 16-2		5.6	44	2.5	2.1	0.6(0.38)	P(NdFeB)	0.654	0.042	0.055	0.008	3(2)	1.03E+18	1.82E+17		0.88
SGU#17		1.6	29	0.5	0.4	0.92	P(NdFeB)	0.6	0.012	0.088	0.029	1.37	7.88E+15	1.71E+17		0.69
Revolver#19-B		7.2	32	3.6	2.8	0.4	H(NdFeB)	0.7	0.045	0.078	0.009	2.7	7.17E+16	3.52E+17		0.63
U#28		16	22	3.52	2.7	0.33(0.33)	P(NdFeB)	0.53	0.045	0.127	0.008	4.93(4.93)	1.39E+16	6.59E+16		1.36
PF-AR 6.5/60																
Bend								1	0.2	0.593	0.036	26	3.90E+13	3.11E+13		
EMPW#NE01-W		16	21	3.36	3(11)	1(0.2)	P(NdFeB)	1.07	1.07	0.268	0.032	15(3)	28(90%)	1.84E+15	2.54E+15	5.52
U#NE03		4	90	3.6	1	0.8	P(NdFeB)	1.57	0.17	0.312	0.029	3	1.29E+16	7.66E+15		3.708
U#NW02		4	90	3.6	1	0.8	P(NdFeB)	1.57	0.17	0.312	0.029	3	1.29E+16	7.66E+15		3.708
U#NW12		4	95	3.8	1	0.8	P(NdFeB)	1.57	0.17	0.312	0.029	3	1.29E+16	7.66E+15		3.912
U#NW14-36		3.6	79	2.8	1	0.8	P(NdFeB)	1.35	0.14	0.338	0.036	2.8	7.69E+15	6.49E+15		3.12
U#NW14-20		2	75	1.5	0.8	0.63	P(NdFeB)	0.75	0.07	0.383	0.038	1.17	7.69E+15	6.49E+15		0.936

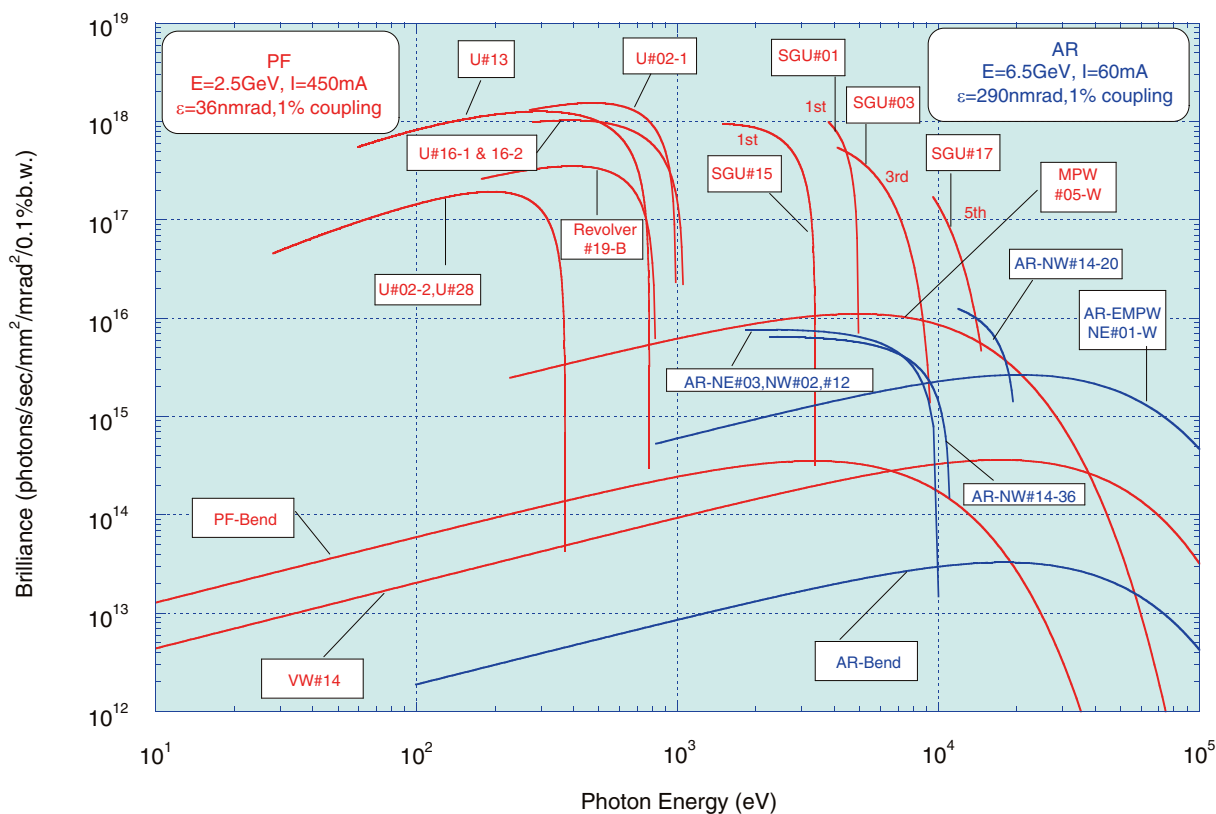


Figure 1: Synchrotron radiation spectra available at the PF ring (2.5 GeV) and the PF-AR (6.5 GeV). Brilliance of the radiation vs. photon energy is denoted by red curves for the insertion devices SGU#01, U#02-1 & 02-2, SGU#03, MPW#05, U#13, VW#14, SGU#15, U#16-1 & 16-2, SGU#17, Revolver#19-B and U#28, and the bending magnets (PF-Bend) at the PF ring. Blue curves denote those for the insertion devices EMPW#NE01, U#NE03, U#NW02, U#NW12, U#NW14-36 and U#NW14-20, and the bending magnets (AR-Bend) at the PF-AR. The name of each source is listed in Table 2. The spectral curve of each undulator (or undulator mode of multipole wiggler) is the locus of the peak of the first harmonic within the allowance range of K parameter. For SGU#01 and SGU#15, the first harmonic regions are shown. For SGU#03, the third harmonic region is shown. For SGU#17, the fifth harmonic region is shown. The spectral curve of Revolver#19 for surface B is shown.

2. Operation Summary

The operation schedule of the PF ring and PF-AR in FY2016 is shown in **Fig. 2**. The statistics of the accelerator's operation for the past decade are shown in **Fig. 3**. The scheduled user times in the PF ring decreased by about 120 hours compared with those in FY2015. In the PF-AR, the times decreased by about 1,680 hours because the construction and commissioning of the new direct beam transport line for the PF-AR were carried out in FY2016.

In the PF ring, more detailed operation statistics and the number of failures from FY2006 to FY2016 are listed in **Table 3** and **Table 4**, and a pie chart of the down time in FY2016 is shown in **Fig. 4**. The mean time between failures (MTBF) was longer than 150 hours due to a large decrease of injection troubles compared with FY2015. The failure rate was 0.6%, which remained at a low value as usual. The user operation for the PF ring was mostly carried out without a top-up injection due to the upgrade of the linac for the SuperKEKB project in FY2016. The helium re-liquefier for the vertical super-

conducting wiggler was replaced in August 2016 and the consumption of liquid helium was improved. However, since leakage in the vacuum chamber frequently occurred, the operation of the wiggler has been suspended since January 2017. The chamber is going to be replaced during the summer shutdown of FY2017.

In the PF-AR, similar statistics are listed in **Table 5** and **Table 6**, and a pie chart of the down time in FY2016 is shown in **Fig. 5**. The MTBF was about 85 hours as usual and the failure rate was 1.7%. In addition, a trouble due to the dust trap occurred only once in FY2016. Stable operation was carried out in FY2016. Construction of the new direct beam transport line for PF-AR since FY2012 was completed, and then the beam commissioning was started on 13th February 2017. The 6.5 GeV electron beam was immediately stored into the ring, and ramp-up was unnecessary thereafter. Then, the vacuum pressure was gradually improved during the commissioning period till 10th March 2017. This result enables us to smoothly resume the user operation in FY2017.

	MON	TUE	WED	THU	FRI	SAT	SUN	MON	TUE	WED	THU	FRI	SAT	SUN	MON	TUE	WED	THU	FRI	SAT	SUN
	9 17	9 17	9 17	9 17	9 17	9 17	9 17	9 17	9 17	9 17	9 17	9 17	9 17	9 17	9 17	9 17	9 17	9 17	9 17	9 17	9 17
Date	4.25	26	27	28	29	30	5.1	2	3	4	5	6	7	8	9	10	11	12	13	14	15
PF																					
AR																					
Date	16	17	18	19	20	21	22	23	24	25	26	27	28	29	30	31	6.1	2	3	4	5
PF																					
AR																					
Date	6	7	8	9	10	11	12	13	14	15	16	17	18	19	20	21	22	23	24	25	26
PF																					
AR																					
Date	27	28	29	30	7.1	2	3	4	5	6	7	8	9	10	11	12	13	14	15	16	17
PF																					
AR																					
Date	10.24	25	26	27	28	29	30	31	11.1	2	3	4	5	6	7	8	9	10	11	12	13
PF																					
AR																					
Date	14	15	16	17	18	19	20	21	22	23	24	25	26	27	28	29	30	12.1	2	3	4
PF																					
AR																					
Date	5	6	7	8	9	10	11	12	13	14	15	16	17	18	19	20	21	22	23	24	25
PF																					
AR																					
Date	1.30	31	2.1	2	3	4	5	6	7	8	9	10	11	12	13	14	15	16	17	18	19
PF																					
AR																					
Date	20	21	22	23	24	25	26	27	28	3.1	2	3	4	5	6	7	8	9	10	11	12
PF																					
AR																					

- PF: PF ring
- AR: PF-AR
- Tuning and ring machine study
- Ring machine study
- Hybrid Mode Operation
- Short maintenance and /or machine study
- B Experiment using SR
- B Bouns

Figure 2: Operation schedule of PF ring and PF-AR in FY2016.

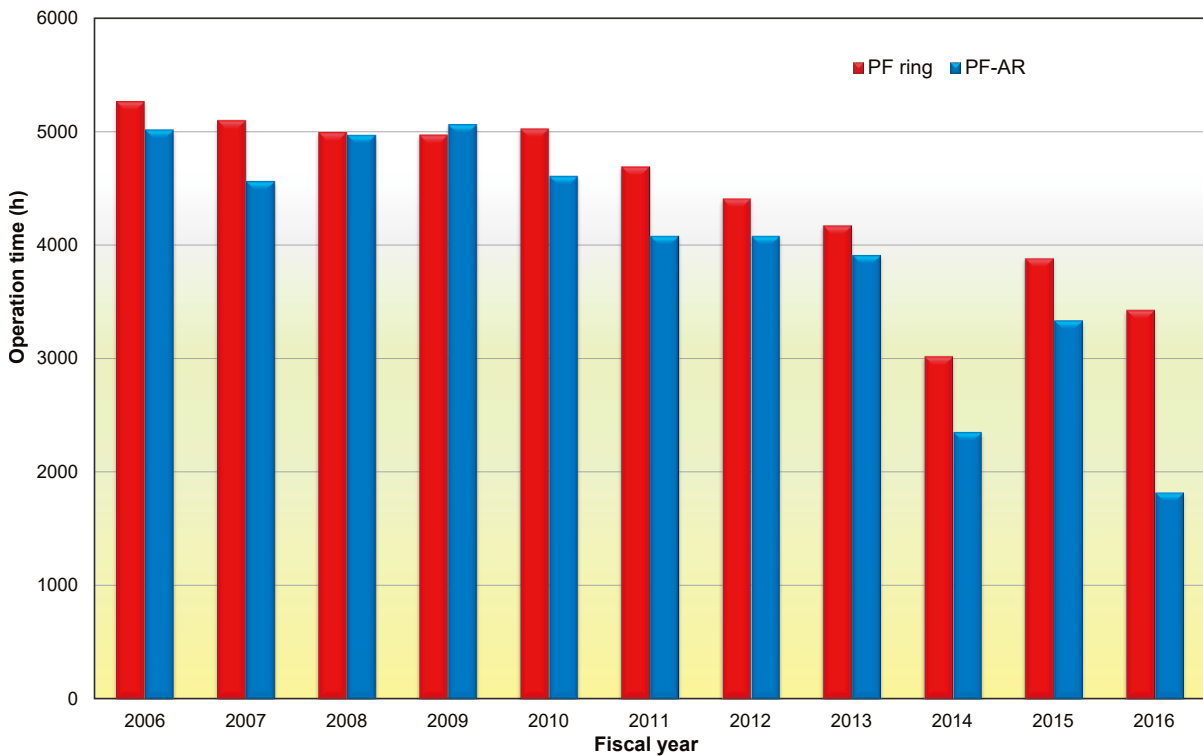


Figure 3: Total operation time for PF ring and PF-AR.

Table 3: Operation statistics for PF ring from FY2006 to FY2016.

Fiscal Year	2006	2007	2008	2009	2010	2011	2012	2013	2014	2015	2016
Total operation time (h)	5272	5104	5000	4976	5064	4728	4416	4176	3024	3888	3432
Scheduled user time (h)	4248	4296	4032	4008	4080	2832	3792	3504	2328	3048	2928
Ratio of user time (%)	80.6	84.2	80.6	80.5	80.6	59.9	85.9	83.9	77.0	78.4	85.3
No. of failures	25	23	18	24	18	18	23	22	15	23	18
Total down time (h)	44.6	91.1	23.8	42.7	29.2	14.9	37.6	52.1	11.4	14.4	17.3
Failure rate (%)	1.0	2.1	0.6	1.1	0.7	0.5	1.0	1.5	0.5	0.5	0.6
MTBF (h)	169.9	186.8	224.0	167.0	226.7	157.3	164.9	159.3	155.2	132.5	162.7
MDT (h)	1.8	4.0	1.3	1.8	1.6	0.8	1.6	2.4	0.8	0.6	1.0

Table 4: Number of failures for PF ring from FY2006 to FY2016.

Fiscal Year	2006	2007	2008	2009	2010	2011	2012	2013	2014	2015	2016
RF	7	4	5	12	13	5	10	8	1	1	1
Magnet	3	2	3	4	0	2	0	2	4	7	7
Injection	2	3	4	0	1	0	0	1	3	6	0
Vacuum	2	1	0	0	0	0	0	0	0	1	2
Dust trap	0	1	0	1	0	0	0	0	0	0	0
Insertion Devices	3	4	3	1	1	4	3	0	1	1	0
Control/ Monitor	1	0	0	3	0	1	6	5	3	3	5
Cooling water	1	0	1	1	0	0	0	0	0	0	0
Safety/ Beamline	2	2	1	2	2	1	1	1	3	2	1
Earthquake	0	2	1	0	0	4	3	1	0	2	2
Electricity	4	4	0	0	1	1	0	4	0	0	0
Total	25	23	18	24	18	18	23	22	15	23	18

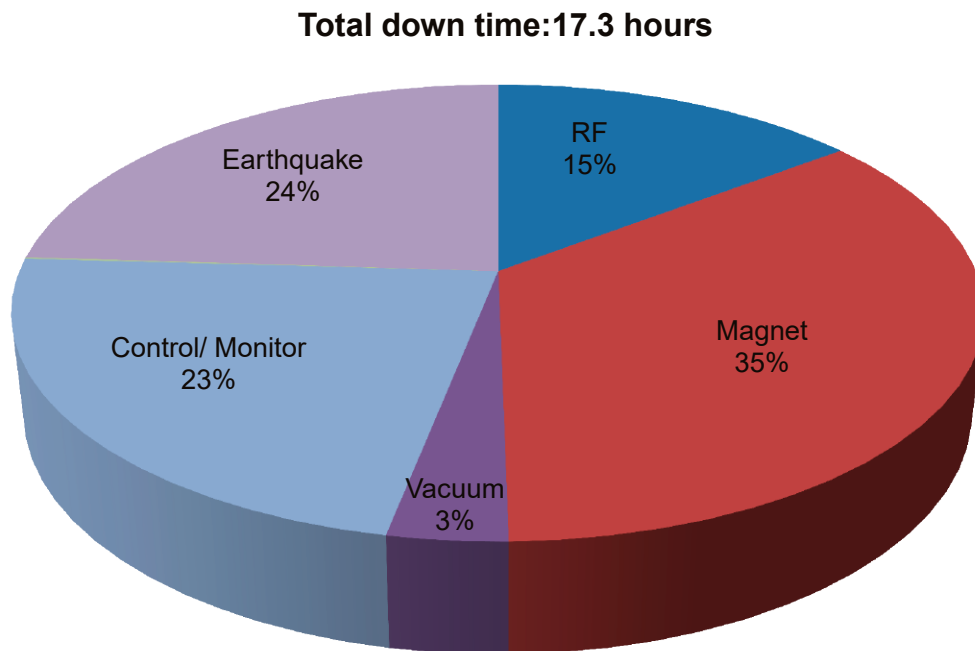


Figure 4: Pie chart of down time for PF ring in FY2016.

Table 5: Operation statistics for PF-AR from FY2006 to FY2016.

Fiscal Year	2006	2007	2008	2009	2010	2011	2012	2013	2014	2015	2016
Total operation time (h)	5016	4561	4969	5063	4608	4080	4080	3912	2352	3336	1821
Scheduled user time (h)	4032	3624	4344	4392	4032	2904	3672	3478	1992	2784	1104
Ratio of user time (%)	80.4	79.5	87.4	86.7	87.5	71.2	90.0	88.9	84.7	83.5	60.6
No. of failures	51	60	40	41	74	49	33	47	22	18	13
Total down time (h)	55.1	45.2	41.7	91.0	73.7	38.7	29.7	99.6	37.0	31.0	18.3
Failure rate (%)	1.4	1.2	1.0	2.1	1.8	1.3	0.8	2.9	1.9	1.1	1.7
MTBF (h)	79.1	60.4	108.6	107.1	54.5	59.3	111.3	74.0	90.5	154.7	84.9
Mean down time (h)	1.1	0.8	1.0	2.2	1.0	0.8	0.9	2.1	1.7	1.7	1.4

Table 6: Number of failures for PF-AR from FY2006 to FY2016.

Fiscal Year	2006	2007	2008	2009	2010	2011	2012	2013	2014	2015	2016
RF	10	1	4	8	10	5	4	5	2	1	3
Magnet	1	1	2	2	10	8	3	4	9	4	5
Injection	3	8	9	1	6	4	3	18	7	1	2
Vacuum	6	2	0	2	1	0	1	0	0	1	1
Dust trap	24	39	15	16	24	20	13	3	2	1	1
Insertion Devices	1	0	0	0	0	0	0	0	0	0	0
Control/ Monitor	0	1	1	1	2	1	2	8	0	0	0
Cooling water	1	0	3	4	4	1	0	2	0	0	0
Safety/ Beamline	4	5	5	7	17	3	4	3	1	8	0
Earthquake	0	1	0	0	0	5	3	1	0	2	1
Electricity	1	2	1	0	0	2	0	3	1	0	0
Total	51	60	40	41	74	49	33	47	22	18	13

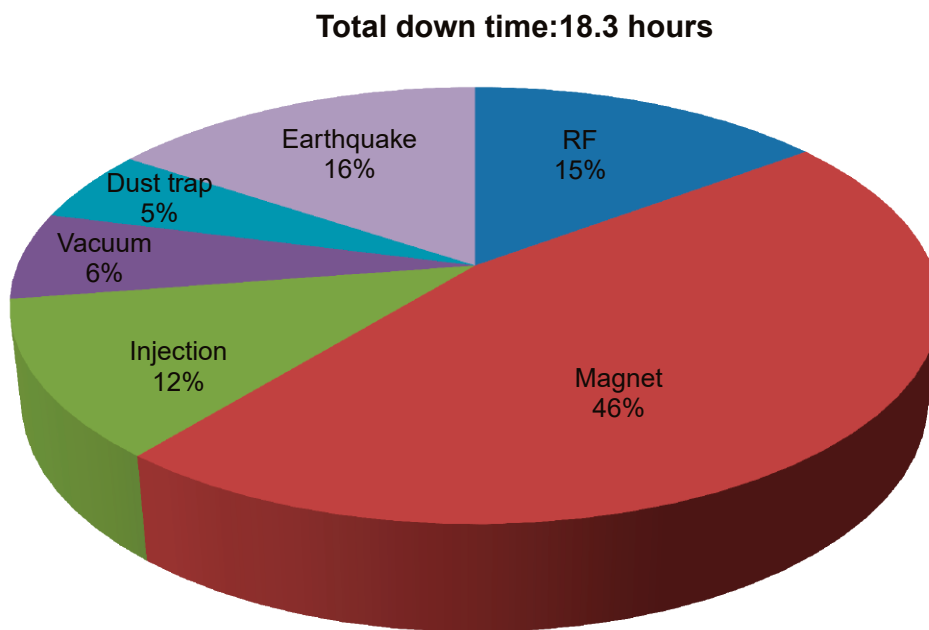


Figure 5: Pie chart of down time for PF-AR in FY2016.

3. Experimental Stations

Fifty-three experimental stations are operated at the PF ring, the PF-AR and the slow positron facility (SPF), as shown in **Figs. 6, 7** and **8**. Thirty-five stations are dedicated to research using hard X-rays, 14 stations

for studies in the VUV and soft X-ray energy regions, and 4 stations for studies using slow positrons. **Tables 7, 8** and **9** summarize the areas of research carried out at the experimental stations at the PF ring, PF-AR and SPF.

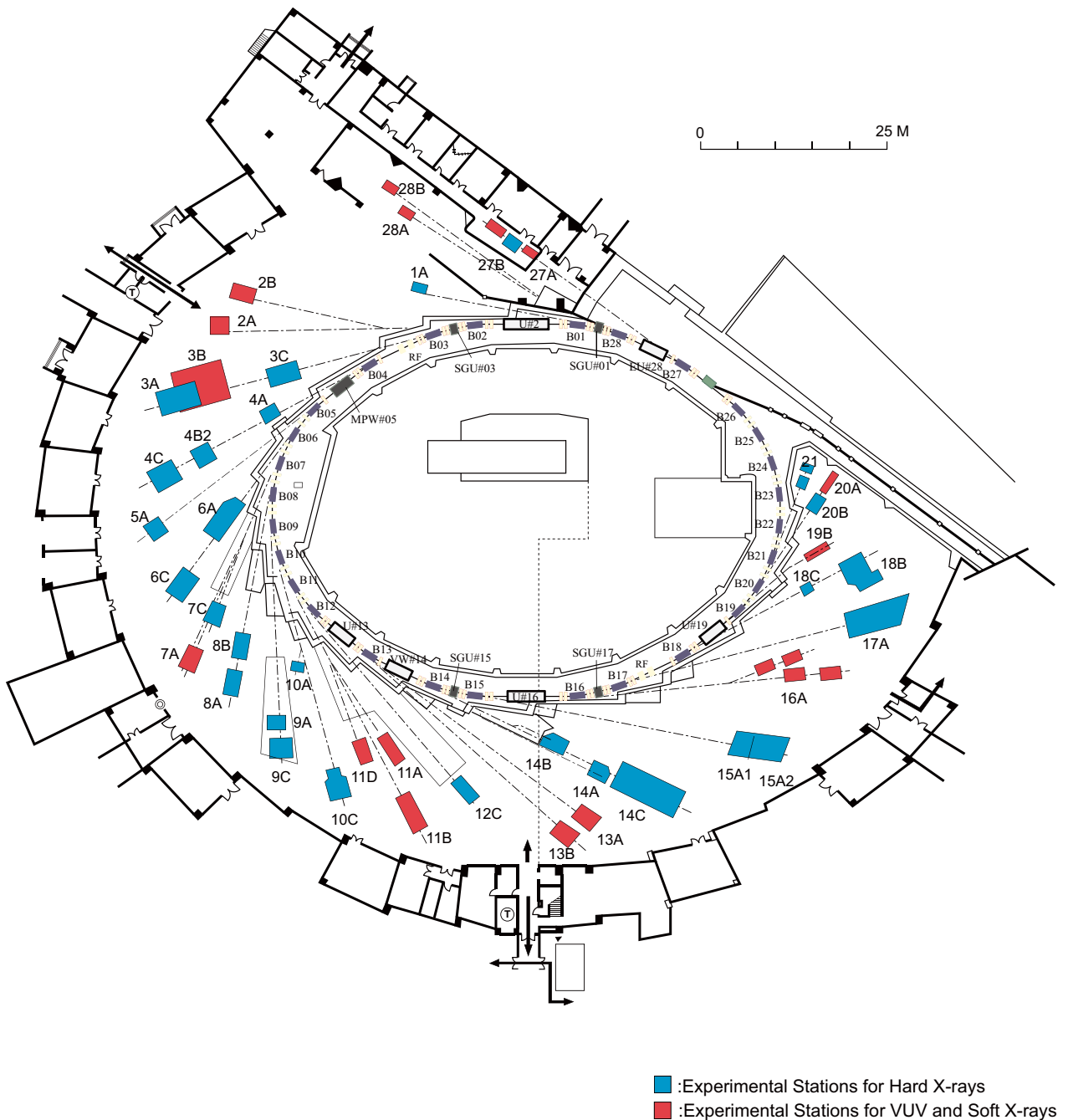


Figure 6: Plan view of the PF experimental hall, showing hard X-ray experimental stations (blue), and VUV and soft X-ray experimental stations (red).

Table 7: List of the experimental stations available for users at the PF ring.

Experimental Station		Person in Charge
BL-1 A	(Short Gap Undulator) Macromolecular crystallography	N. Matsugaki
BL-2 A B	(Variable Polarization Undulator for VUV and planer undulator for SX) High-resolution VUV-SX beamline for angle-resolved photoemission spectroscopy High-resolution VUV-SX spectroscopies	H. Kumigashira H. Kumigashira
BL-3 A B C	(A: Short Gap Undulator) X-ray diffraction for material structural science VUV and soft X-ray spectroscopy (♣) Characterization of X-ray optical elements/White X-ray magnetic diffraction	H. Nakao K. Edamoto [Rikkyo Univ.], J. Yoshinobu [The Univ. of Tokyo], K. Mase K. Hirano
BL-4 A B2 C	Trace element analysis, X-ray microprobe (♣) High resolution powder diffraction (♣) X-ray diffraction for material structural science	Y. Takahashi [The Univ. of Tokyo], M. Kimura, Y. Niwa H. Uekusa [Tokyo Inst. of Tech.], H. Nakao H. Nakao
BL-5 A	(Multipole Wiggler) Macromolecular crystallography	N. Matsugaki
BL-6 A C	Small-angle X-ray scattering Macromolecular crystallography (♣)	N. Igarashi M. Okube [Tohoku Univ.], H. Kawata
BL-7 A C	Soft X-ray spectroscopy (♣) X-ray spectroscopy and diffraction	J. Okabayashi [RCS], K. Amemiya H. Sugiyama
BL-8 A B	Weissenberg camera for powder/Single-crystal measurements under extreme conditions Weissenberg camera for powder/Single-crystal measurements under extreme conditions	H. Sagayama H. Sagayama
BL-9 A C	XAFS XAFS	H. Abe H. Abe
BL-10 A C	X-ray diffraction and scattering (♣) Small-angle X-ray Scattering	A. Yoshiasa [Kumamoto Univ.], R. Kumai N. Shimizu
BL-11 A B D	Soft X-ray spectroscopy Soft X-ray spectroscopy Characterization of optical elements used in the VSX region	Y. Kitajima Y. Kitajima K. Mase
BL-12 C	XAFS	H. Nitani

Experimental Station		Person in Charge
BL-13 A/B	(Variable Polarization Undulator) VUV and soft X-ray spectroscopies with circular and linear polarization	K. Mase
BL-14 A B C	(Vertical Wiggler) Crystal structure analysis and detector development High-precision X-ray optics Medical applications and general purpose (X-ray)	S. Kishimoto K. Hirano K. Hyodo
BL-15 A1 A2	(Short Gap Undulator) Semi-microbeam XAFS High brilliance small-angle X-ray scattering	Y. Takeichi N. Shimizu
BL-16 A	(Variable Polarization Undulator) Soft X-ray spectroscopies with circular and linear polarization	K. Amemiya
BL-17 A	(Short Gap Undulator) Macromolecular crystallography	Y. Yamada
BL-18 B C	Multipurpose monochromatic hard X-ray station (◆) High pressure X-ray powder diffraction (DAC) (♠)	R. Prasad Giri [SINP], R. Kumai H. Kagi [The Univ. of Tokyo], T. Kikegawa
BL-19 B	Test beamline	H. Nakao
BL-20 A B	VUV spectroscopy (◇) White & monochromatic X-ray topography and X-ray diffraction experiment	N. Kouchi [Tokyo Inst. of Tech], J. Adachi H. Sugiyama
BL-27 A B	(Beamline for radioactive samples) Radiation biology, soft X-ray photoelectron spectroscopy Radiation biology, XAFS	N. Usami N. Usami
BL-28 A B	(Variable Polarization Undulator) High-resolution angle-resolved photoemission spectroscopy with circular and linear polarization High-resolution VUV spectroscopies with circular and linear polarization	K. Ono K. Ono

- ♠ User group operated beamline
◆ External beamline
◇ Operated by University

RCS: Research Center for Spectrochemistry, the University of Tokyo
SINP: Saha Institute of Nuclear Physics

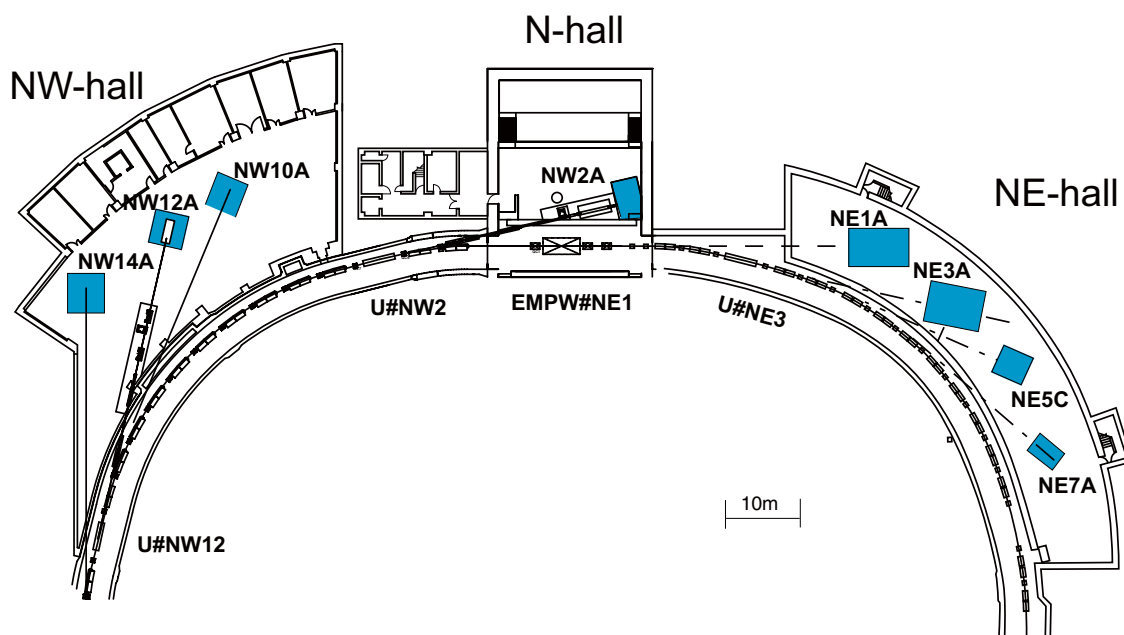


Figure 7: Plan view of the beamlines in the PF-AR north-east, north, and north-west experimental halls.

Table 8: List of the experimental stations at the PF-AR.

Experimental Station		Person in Charge
AR-NE1	(Multipole Wiggler)	
A	Laser-heating high pressure X-ray diffraction and nuclear resonant scattering (DAC)	T. Kikegawa
AR-NE3	(In-vacuum Undulator)	
A	Macromolecular crystallography	Y. Yamada
AR-NE5		
C	High pressure and high temperature X-ray diffraction (MAX-80)	T. Kikegawa
AR-NE7		
A	High pressure and high temperature X-ray diffraction (MAX-III) (♥), X-ray imaging	K. Hyodo, A. Suzuki [Tohoku Univ.]
AR-NW2	(In-vacuum Type Tapered Undulator)	
A	Time-resolved Dispersive XAFS/XAFS/X-ray Diffraction	Y. Niwa
AR-NW10		
A	XAFS	H. Nitani
AR-NW12	(In-vacuum Type Tapered Undulator)	
A	Macromolecular crystallography	M. Hikita
AR-NW14	(In-vacuum Undulator)	
A	Time-resolved X-ray diffraction, scattering and absorption	S. Nozawa

♥ User group operated experimental equipment

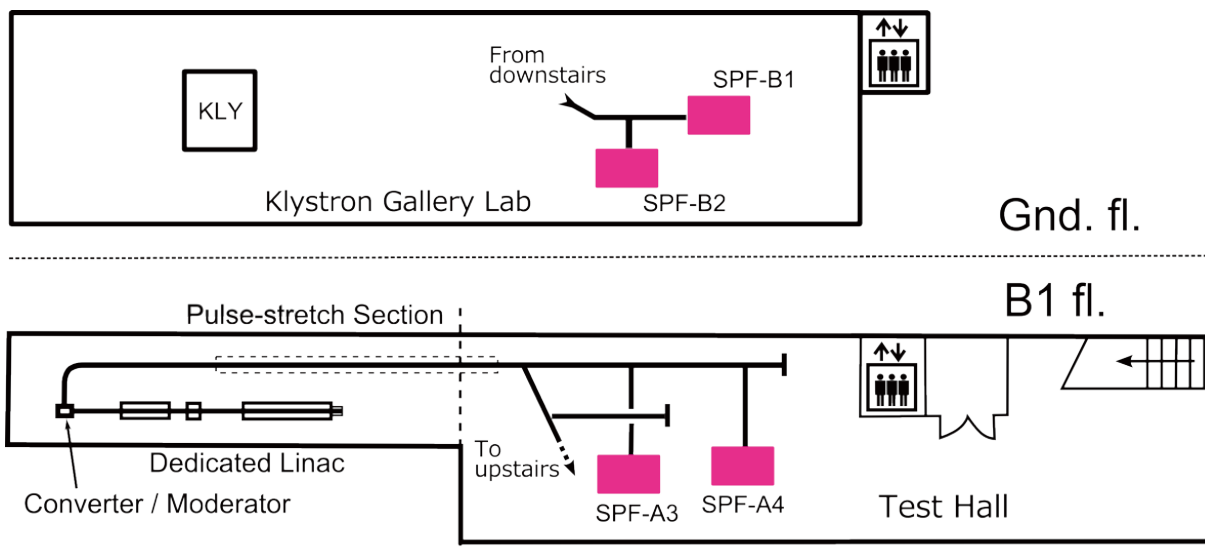


Figure 8: View of the beamlines in the Slow Positron Facility.

Table 9: List of the experimental stations in the Slow Positron Facility.

Experimental Station		Person in Charge
SPF-A3	Total-reflection high-energy positron diffraction	T. Hyodo
SPF-A4	Low-energy positron diffraction	T. Hyodo
SPF-B1	General purpose (Positronium negative ion)	T. Hyodo
SPF-B2	Positronium time-of-flight	T. Hyodo

4. Summary of User Proposals

The Photon Factory accepts experimental proposals submitted by researchers mainly at universities and research institutes inside and outside Japan. The PF Program Advisory Committee (PF-PAC) reviews the proposals, and the Advisory Committee for the Institute of Materials Structure Science formally approves those that are favorably recommended. The number of accepted proposals over the period 2005–2016 is shown in Table 10, where S1/S2, U, G, P, MP denote Special, Urgent, General, Preliminary, and Multi-Probe proposals, respectively. Category T is a new type of proposal for supporting researches by PhD students. Category MP is also a new type of proposal in which no less than two of the four beams, synchrotron radiation at the PF, slow positron at the Slow Positron Facility, and neutron and muon beams at the Materials and Life Science Experimental Facility (MLF) in J-PARC, are required to be used, as a multi-probe experiment.

Category C is a proposal to carry out a joint experiment between KEK and a research institute including a private company. Category I is a non-proprietary proposal for integrated promotion of social system reform and research and development, supported by the Ministry of Education, Culture, Sports, Science and Technology. Category V is a non-proprietary grant-aided proposal that has already been reviewed and approved for a research grant; beam time for these proposals is allocated with high priority, and the applicants are required to pay the regulation fees for the beam time. Category Y is a proprietary proposal; the applicants are required to pay the regulation fees for the beam time. The number of current G-type proposals each year has exceeded 800 for the past few years. In addition to these proposals, 50 projects in the Platform for Drug Discovery, Informatics, and Structural Life Science were performed at the PF in FY2016. A full list of the proposals effective in FY2016 and their scientific output can be found in the Photon Factory Activity Report (<http://www2.kek.jp/imss/pf/science/publ/acrpubl.html>).

Table 10: Number of proposals accepted for the period 2005–2016.

Category	FY-2005	2006	2007	2008	2009	2010	2011	2012	2013	2014	2015	2016
S1	0	1	0	0	0	0	0	0	0	0	0	0
S2	3	6	1	4	6	3	2	4	5	4	7	6
U	0	1	7	3	2	2	0	4	1	0	0	0
G	310	386	403	402	397	407	415	454	447	407	361	372
P	10	22	14	14	14	16	11	18	18	5	16	10
T										6	4	3
MP											4	-
C	28	25	24	18	12	15	19	20	20	25	24	37

S-type proposals consist of two categories, S1 and S2. S1 proposals are self-contained projects of excellent scientific quality, and include projects such as the construction and improvement of beamlines and experimental stations which will be available for general users after the completion of the project. S2 proposals are superior-grade projects that require the full use of synchrotron radiation or long-term beam time. Proposals are categorized into five scientific disciplines, and reviewed by the five subcommittees of PF-PAC: 1) electronic structure, 2) structural science, 3) chemistry and materials, 4) life science I (protein crystallography), and 5) life science II (including soft matter science). **Figure 9** shows the distribution by research field of the proposals accepted by the subcommittees in FY2016.

The number of users, for all types of proposals, now exceeds 3,010. Although the number of experimental stations has decreased, the approved scientific proposals and number of users have increased annually, as shown in **Fig. 10**. This indicates a high and increasing demand for synchrotron radiation and can be attributed to continuous improvements in the storage rings, beamlines, and experimental stations. The synchrotron has become one of the most important research tools for carrying out advanced science experiments and development. About 22% of the proposals are conducted by new spokespersons, which indicates that the Photon Factory is open to public academic scientists. **Figure 11** shows the distribution of users by institutional position. Over three-quarters of the users belong to universities, of whom approximately 73% are associated with national universities. Over two-thirds of the national university

users are graduate and undergraduate students; this indicates that the Photon Factory plays an important role in both research and education. The geographical distribution of the Photon Factory users is shown in **Fig. 12** and **Fig. 13**, which also indicates the immense contribution of the Photon Factory to research and education throughout Japan. The registered number of papers published in 2016 based on experiments at the PF was 407 at the time of this writing (July 1st, 2017). In addition, 34 doctoral and 94 master theses have been presented.

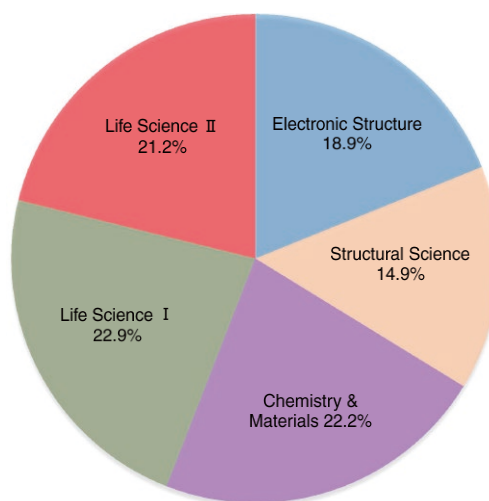


Figure 9: Distribution by scientific field of experimental proposals accepted in FY2016.

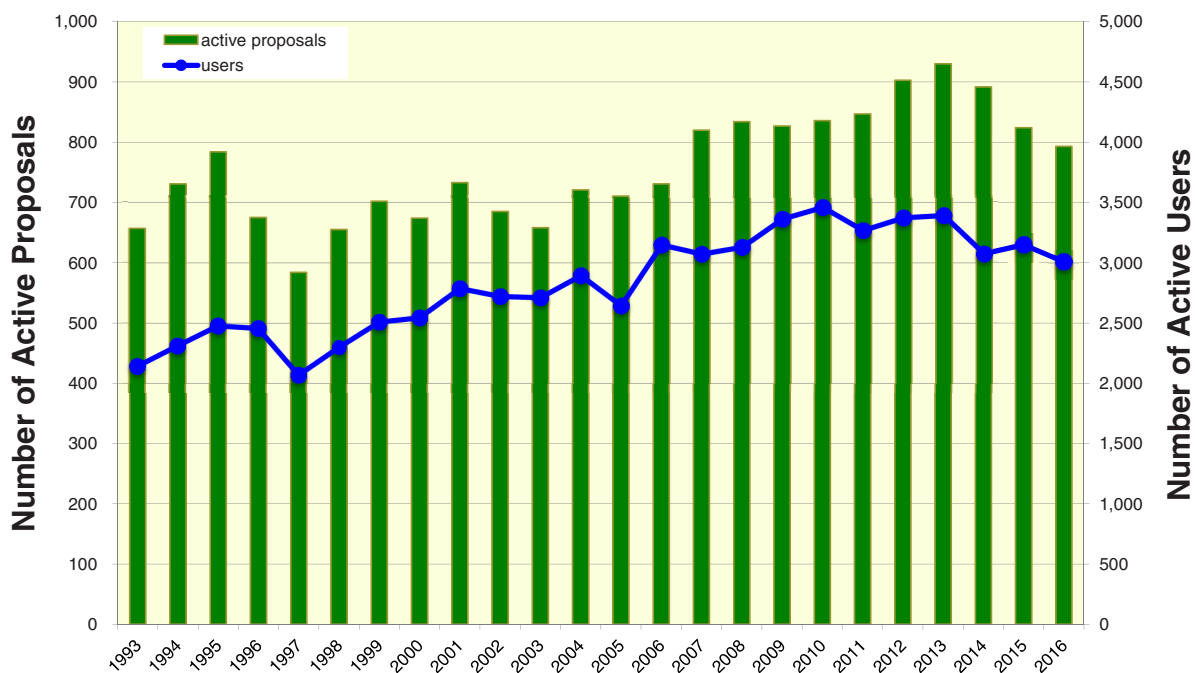


Figure 10: Number of registered PF users and scientific proposals over the period 1993–2016.

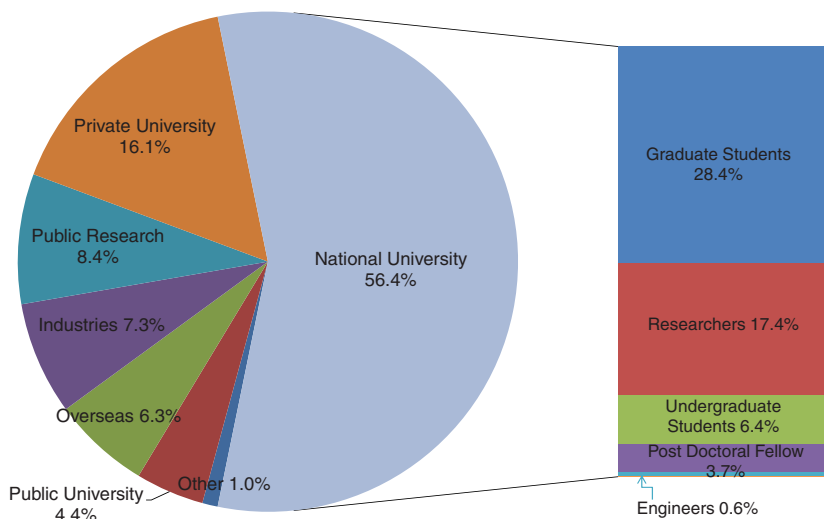


Figure 11: Distribution of users by institution and position.

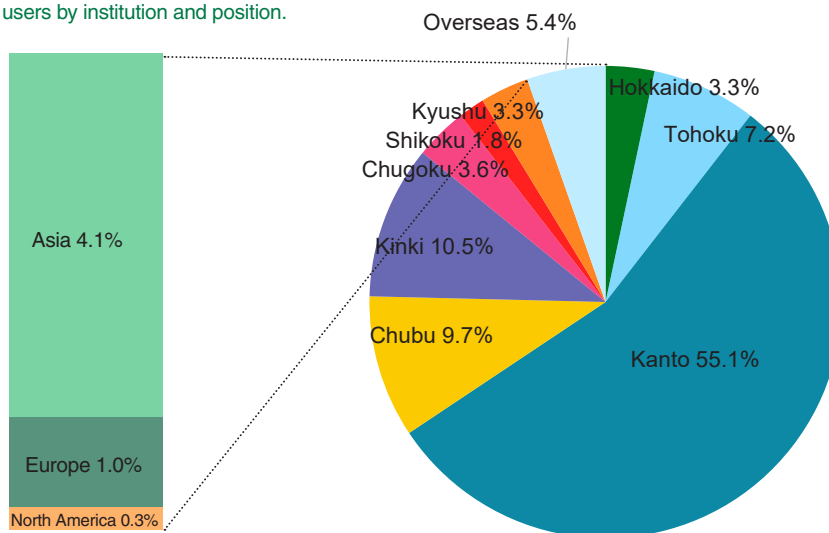


Figure 12: Regional distribution of spokespersons of proposals accepted in FY2016. We corrected the pie chart on 2019/09/02.

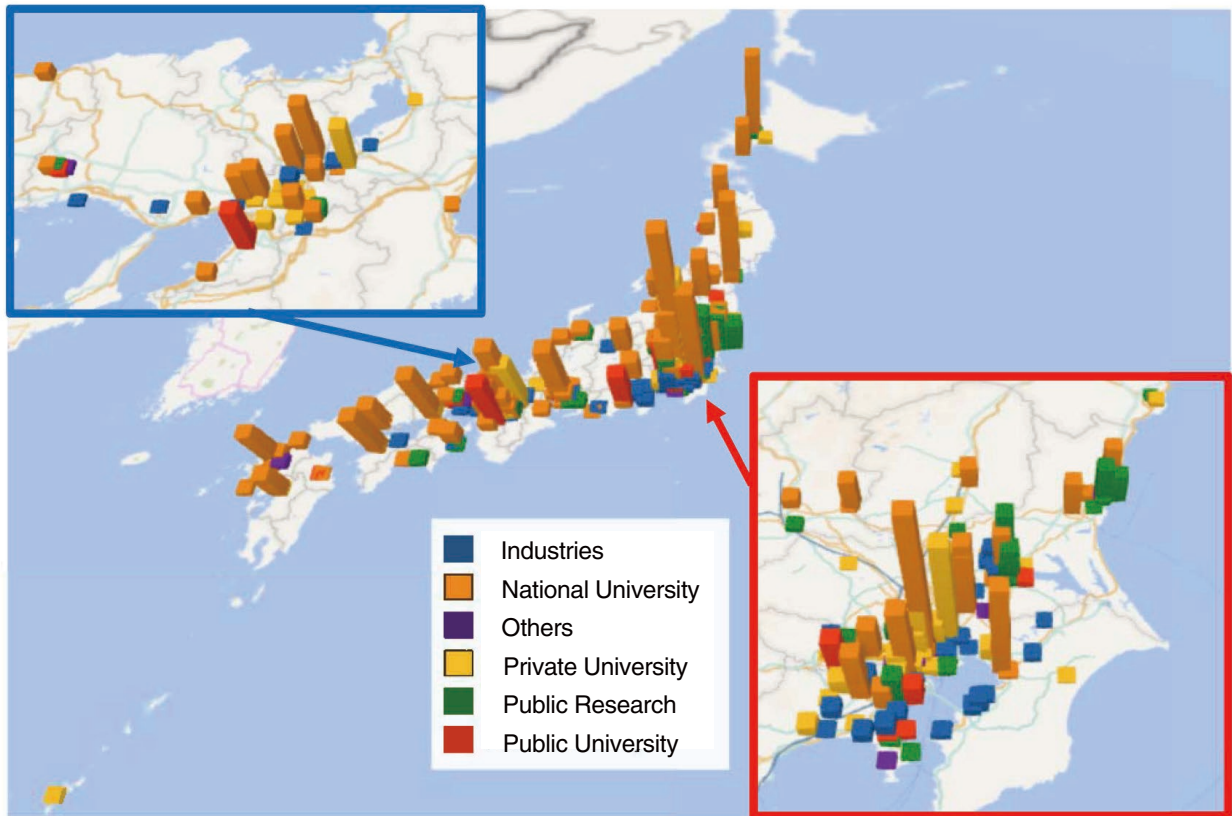


Figure 13: Geographical distribution of Photon Factory users in FY2016 (domestic users only).